Enhancement of perpendicular magnetic anisotropy and spin-orbit torque in Ta/Pt/Co/Ta multi-layered heterostructures through interfacial diffusion

Cite as: Appl. Phys. Lett. **114**, 042404 (2019); https://doi.org/10.1063/1.5064643
Submitted: 06 October 2018 . Accepted: 13 January 2019 . Published Online: 31 January 2019

Rui Wang, Zhengyu Xiao, Huihui Liu, Zhiyong Quan, Xiao Zhang, Meimei Wang, Mingzhong Wu, and Xiaohong Xu

Applied Physics Letters ARTICLE scitation.org/journal/apl

Enhancement of perpendicular magnetic anisotropy and spin-orbit torque in Ta/Pt/Co/Ta multi-layered heterostructures through interfacial diffusion

Cite as: Appl. Phys. Lett. **114**, 042404 (2019); doi: 10.1063/1.5064643
Submitted: 06 October 2018 · Accepted: 13 January 2019 · Published Online: 31 January 2019

Rui Wang,[1,a)] Zhengyu Xiao,[1,2,a)] Huihui Liu,[1] Zhiyong Quan,[1,2,b)] Xiao Zhang,[1] Meimei Wang,[1] Mingzhong Wu,[3] and Xiaohong Xu[1,2,b)]

AFFILIATIONS

[1] Key Laboratory of Magnetic Molecules and Magnetic Information Materials of Ministry of Education, the School of Chemistry and Materials Science, Shanxi Normal University, Linfen 041004, China
[2] Research Institute of Materials Science, Shanxi Normal University, Linfen 041004, China
[3] Department of Physics, Colorado State University, Fort Collins, Colorado 80523, USA

[a)] **Contributions:** R. Wang and Z. Xiao contributed equally to this work.
[b)] **Authors to whom correspondence should be addressed:** quanzy@sxnu.edu.cn and xuxh@sxnu.edu.cn

ABSTRACT

Heavy metal/ferromagnetic metal bi-layered structures that exhibit both strong perpendicular magnetic anisotropy (PMA) and large spin-orbit torque (SOT) efficiency have high potential in high-density, low-power memory, and logic device applications. Here, we report the enhancement of PMA and SOT in Ta/Pt/Co/Ta multi-layered heterostructures through interfacial diffusion. The structures can exhibit PMA fields of 9100 Oe at 300 K and 14100 Oe at 10 K and an effective spin Hall angle (SHA) of 0.61 ± 0.03 at 300 K. These values are larger than the corresponding values reported previously for similar heterostructures. The current-induced magnetization switching was demonstrated. The critical switching current density is on the order of 10^6 A/cm^2, and the corresponding switching efficiency is higher than that reported for similar structures. X-ray absorption spectroscopy and high-angle annular dark-field scanning transmission electron microscopy analyses suggest a strong correlation between the observed PMA and SOT enhancement and the interfacial diffusion during the sputtering growth of the samples. It is very likely that the interfacial diffusion gives rise to enhanced spin-orbit coupling at the interface, while the latter results in enhancement in the PMA, SHA, and switching efficiency in the structure.

Recent years have witnessed rather significant interest in studying spin-orbit torque (SOT) in heavy metal (HM)/ferromagnetic metal (FM) bi-layered structures.[1,2] Via either the spin Hall effect (SHE) or the Rashba effect, a charge current in the HM layer can produce a SOT that can induce magnetization switching,[3–6] domain-wall motion,[7,8] or magnetic oscillation[9,10] in the FM layer. Such SOT-induced magnetization dynamics can be used to develop novel logic and memory devices that may consume significantly lower power than conventional devices.[2] For SOT-based high-density memory, the realization of robust perpendicular magnetic anisotropy (PMA) in the HM/FM heterostructure is essential to maintain a sufficiently large energy barrier against thermal fluctuation.[11,12] Recent studies show that one can enhance PMA in CoFeB/MgO bi-layers through controlled nitrogen doping to Ta underlayers,[13] and interfacial PMA can be increased by inserting ultrathin W or HfO_2 layers.[14,15]

Meanwhile, it is very important to reduce the critical switching current density J_c in SOT-based devices in order to achieve low power consumption. A key to minimizing J_c in SHE-based devices is to maximize the spin Hall angle (SHA) as J_c is usually given by $J_c = 2eM_S t_{FM}\left(H_{an}^0/2 - H_{ext}/\sqrt{2}\right)/\hbar\Theta_{SH}$.[16–18] In this equation, H_{ext} is an external magnetic field collinear with the current, e is the elementary charge, $\hbar$ is the reduced Planck

constant, Θ_{SH} is the effective SHA, M_S is the saturation magnetization, t_{FM} is the FM layer thickness, and H_{an}^0 is the effective PMA field of the FM layer. One of the efficient methods to obtain a large effective SHA is to sandwich a FM layer with two HM layers whose SHAs have opposite signs, and large Θ_{SH} values have been reported previously.[19,20]

It has been reported very recently that the interface in a HM/FM heterostructure strongly affects both the PMA and SHA properties. On one hand, experimental studies have shown that the addition of a ultrathin Hf or Cr layer in between the HM and FM layers can improve interfacial coupling or spin transparency or suppress oxidation at the HM/FM interface, thereby enhancing the SOT and/or the PMA.[14,21–24] On the other hand, a very recent theoretical work predicts that the HM/FM interface has a significant contribution to the SHE,[25] and the interfacial SHA can be about 25 times larger than the bulk value in HM/FM bi-layers. Understanding of the effects of the interfaces on the SOT and PMA properties in HM/FM systems is crucial for the future development of efficient SOT devices.

Here, we report that one can also take the advantage of interfacial diffusion to notably improve PMA and SOT in HM/FM heterostructures. We grew Ta/Pt/Co/Ta multi-layered structures via magnetron sputtering at room temperature. In comparison with similar structures reported previously, our heterostructures show an enhanced PMA field ($H_{an}^0 = 9150$ Oe at 300 K) and a larger effective SHA value ($\Theta_{SH}^{eff} = 0.61 \pm 0.03$). In fact, the effective SHA value is the largest value reported so far for Pt(Ta)-based systems.[3,19,20] We believe that this large SHA is not only because of the use of two HM layers with opposite SHA signs but also partially due to enhanced interfacial spin-orbit coupling (SOC) that is attributed to the interfacial diffusion between the Co and HM layers during the sputtering growth. The enhanced SOC was confirmed by X-ray absorption spectroscopy (XAS) analyses, while the interfacial diffusion was confirmed by high-angle annular dark-field scanning transmission electron microscopy (HAADF-STEM) measurements. Thanks to the large SHA, efficient SOT switching was demonstrated in the Ta/Pt/Co/Ta structure; the switching current density could be as low as 10^6 A/cm^2 in the presence of an in-plane external field of 400 Oe, which corresponds to a switching efficiency higher than that in similar structures.[19,20,26] Our results show that HM/FM structures with very large PMA and SHA values can be obtained through interface engineering. Thus, we believe that our work provides important implications for the future development of SOT-based spintronic devices.

Ta(2)/Pt(5)/Co(0.9)/Ta(2) multi-layered (thickness in nm) structures were prepared by DC magnetron sputtering from 2-in. targets on thermally oxidized Si substrates. The base pressure of the sputtering system was 5×10^{-9} Torr. Four samples were prepared. The Co layers in those samples were grown at different Ar pressures ($P_{Ar} = 5$, 10, 20, and 25 mTorr), while the HM layers were grown at $P_{Ar} = 5$ mTorr. The magnetic properties of the samples were measured with a superconducting quantum interference device (SQUID) magnetometer with in-plane and out-of-plane magnetic fields. The out-of-plane hysteresis loops measured at 300 K are shown in Fig. S1 in the supplementary material. One can see that the film grown at $P_{Ar} = 20$ mTorr (labeled as Ta/Pt/Co/Ta-20) shows stronger PMA and higher coercivity. Thus, we primarily focus on the results of the Ta/Pt/Co/Ta-20 sample in this paper. Using standard photolithography and Ar ion etching, the samples were patterned into Hall bars with a dimension of 10×100 μm^2 for Hall voltage measurements [see Fig. 1(a)]. A physical property measurement system (PPMS) was used for transport measurements at temperatures ranging from 10 K to 350 K. Harmonic Hall voltage measurements were also performed to obtain the effective SOT fields and the SHA value at 300 K. X-ray absorption spectroscopy (XAS) measurements were made using the Beamline BL08U1A and BL12-a. Cross-sectional high-resolution structural characterization was performed using transmission electron microscopy (TEM). HAADF-STEM and the energy-dispersive X-ray spectroscopy (EDX) line scan were performed to study the interfaces.

Figure 1 presents the data measured on the Ta/Pt/Co/Ta-20 sample. Figure 1(b) shows the in-plane and out-of-plane magnetic hysteresis loops measured at 300 K. One can see that the out-of-plane direction (the z axis) is the easy magnetization axis, and the out-of-plane loop shows high squareness and high remanence. Figure 1(c) shows the anomalous Hall effect (AHE) resistance (R_{AHE}) loops of the Ta/Pt/Co/Ta-20 sample measured at different temperatures under a perpendicular magnetic field, using the configuration shown in Fig. 1(a). The loops indicate the presence of strong PMA in the Co layer over the entire temperature range of 10–300 K. The coercive field (H_c) decreases quickly with an increase in temperature, which is very likely due to the thermal activation of domain wall motion at high temperatures. The R_{AHE} value increases slightly with the temperature due to strong electron-magnon scattering at high temperatures.[27] Figure 1(d) shows the current-induced perpendicular magnetization switching curves in the Ta/Pt/Co/Ta-20 sample at 300 K. The square loops confirm that a current-generated SOT drives

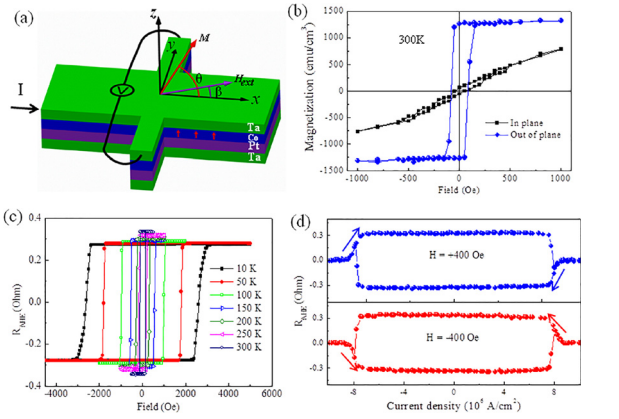

FIG. 1. (a) Configuration for transport measurements on a Ta/Pt/Co/Ta multi-layered Hall bar structure. The external magnetic field (H_{ext}) and the charge current (I, along the x axis) are indicated. β is the angle between H_{ext} and the x axis. θ is the angle between the magnetization vector $\boldsymbol{M}$ and the x axis. (b) In-plane and out-of-plane magnetic hysteresis loops measured on the Ta/Pt/Co/Ta-20 sample at 300 K. (c) Anomalous Hall resistance loops measured on the Ta/Pt/Co/Ta-20 sample with a perpendicular magnetic field at different temperatures, as indicated. (d) Current-induced magnetization switching of the Ta/Pt/Co/Ta-20 sample under a positive external field ($\beta = 0°$) and a negative external field ($\beta = 180°$).

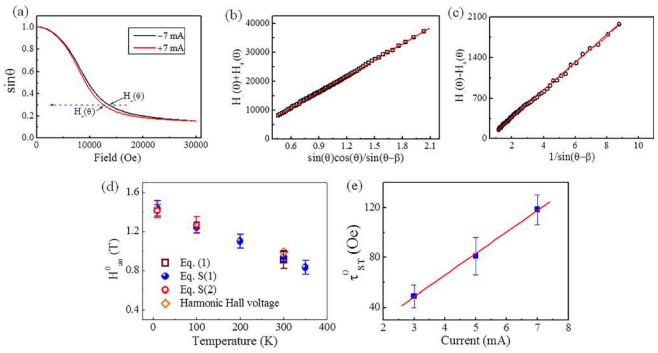

FIG. 2. (a) Normalized anomalous Hall resistance ($\sim\sin\theta$) of the Ta/Pt/Co/Ta-20 sample as a function of the strength of a nearly in-plane magnetic field ($\beta = 7°$) under ± 7 mA excitation currents. (b) $H_-(\theta)+H_+(\theta)$ vs. $\sin(\theta)\cos(\theta)/\sin(\theta-\beta)$ data and a linear fit to Eq. (1). (c) $H_-(\theta)-H_+(\theta)$ vs. $1/\sin(\theta-\beta)$ data and a linear fit to Eq. (2). (d) H^0_{an} as a function of temperature, obtained through fitting the data in (b), Figs. S2, and 3(a), using Eqs. (1), S(1), and S(2). (e) τ^0_{ST} as a function of excitation current and a linear fit.

the magnetization switching along the out-of-plane direction. The polarity of the switching loop reverses upon the flip of the in-plane field direction, which is consistent with SHE-induced SOT switching in previous studies.[3,4,28] The switching critical current density is about 7.8×10^6 A/cm^2, which is either lower than or comparable to that in other similar structures.[3,4] If we follow the discussions in Ref. 25 and define the switching efficiency as $\eta = (H^0_{an} - H_{ext})/J_c$, we obtain an efficiency of 1.1×10^{-7} Oe·m^2/A. This value is significantly higher than that reported previously for similar heterostructures.[19,20]

In order to quantitatively determine the PMA field, SOT, and SHA values in the Ta/Pt/Co/Ta-20 sample, we made use of the direct current (DC) Hall method[3,29,30] and conducted Hall measurements over 10–350 K using the configuration shown in Fig. 1(a). In our measurements, the in-plane magnetic field was applied to the sample within the z-x plane at a small angle of $\beta \approx 7°$ with respect to the x axis. The direction of the magnetization vector (**M**) of the Co layer depends on (1) the SOT due to the SHE-induced spin current, (2) the external field H_{ext}, and (3) the effective PMA field H_{an}. The magnetization angle with respect to the sample plane (θ) is determined by measuring the AHE resistance, i.e., $\sin\theta = R_{AHE}/R_0$, where R_0 is the Hall resistance at $\theta = 90°$. The equilibrium equation for **M** is $\vec{\tau}_{tot} = \vec{\tau}_{ST} + \vec{\tau}_{ext} + \vec{\tau}_{an} = 0$, where $\vec{\tau}_{ST} = \vec{\tau}^0_{ST}(\hat{m}\times(\hat{\sigma}\times\hat{m}))$ is the SOT per unit moment, $\vec{\tau}_{ext}$ is the torque of the external magnetic field, and $\vec{\tau}_{an}$ is the torque of the PMA field. Note that in the SOT, $\tau^0_{ST} = \hbar J_C/2eM_s t_{FM}$ is the torque amplitude, $\hat{m}$ is the unit vector along **M**, and $\hat{\sigma}$ denotes the polarization direction of the spin current J_S. The equilibrium equation can be rewritten in a scalar form along the y axis[8] as $\tau^0_{ST} + H_{ext}\sin(\theta-\beta) - H^0_{an}\sin\theta\cos\theta = 0$. Below, we use this scalar equation to determine H^0_{an} and τ^0_{ST}.

Figure 2(a) shows the normalized anomalous Hall resistance, namely, $\sin(\theta)=R_{AHE}/R_0$, of the Co layer as a function of H_{ext} under the currents of ± 7 mA. We can write down two equations, one for the positive current involving $H_+(\theta)$ and the other for the negative current involving $H_-(\theta)$. From those two equations, we obtain

$$[H_-(\theta) + H_+(\theta)] = 2H^0_{an}\sin\theta\cos\theta/\sin(\theta-\beta), \quad (1)$$

$$[H_-(\theta) - H_+(\theta)] = 2\tau^0_{ST}/\sin(\theta-\beta). \quad (2)$$

We can then determine H^0_{an} and τ^0_{ST} by using Eqs. (1) and (2) to fit the $H_-(\theta)+H_+(\theta)$ vs. $\sin(\theta)\cos(\theta)/\sin(\theta-\beta)$ data and the $H_-(\theta)-H_+(\theta)$ vs. $1/\sin(\theta-\beta)$ data, respectively.[3,4]

Figure 2(b) shows $H_-(\theta)+H_+(\theta)$ as a function of $\sin(\theta)\cos(\theta)/\sin(\theta-\beta)$ measured at 300 K. The value of β in our experiments was fixed at 7°. The fitting using Eq. (1) yields $H^0_{an} = 9150$ Oe. Using the other methods (see S2 in the supplementary material), we obtained H^0_{an} values at different temperatures and present them in Fig. 2(d). These values are larger than those presented in previous studies.[31,32] Figure 2(c) presents $H_-(\theta)-H_+(\theta)$ as a function of $1/\sin(\theta-\beta)$ measured at 300 K. τ^0_{ST} can be obtained by using Eq. (2) to fit the data in Fig. 2(c). Figure 2(e) presents fitting-yield τ^0_{ST} values for three different currents. Based on these values, we can then use $\Theta_{SH} = J_S/J_e = 2eM_S t_{Co}\tau^0_{ST}/J_e\hbar$ to evaluate the SHA value. Note that t_{Co} is the thickness of the Co layer, and $M_s \approx 1300$ emu/cm^3 is the saturation magnetization of the Co layer [see Fig. 1(b)]. This analysis yields an effective SHA value of 0.61 ± 0.03 at 300 K in our Ta/Pt/Co/Ta-20 structure. This value is notably larger than the values reported previously for double HM-based heterostructures, including 0.34 in Ref. 19, 0.45 in Ref. 20, and 0.41 in Ref. 24.

We also performed harmonic Hall voltage measurements in the patterned Hall bars to evaluate the current-induced SOT fields and the SHA value. A low-frequency alternating current with a frequency of 13.7 Hz and an amplitude of 3 mA was applied. The first and second harmonic Hall voltages were measured using two lock-in amplifiers.[33] The magnetic field was applied along the current direction with a small angle of about 4° away from the film plane. The measurements were performed in longitudinal (H//I) and transverse (H ⊥ I) configurations to estimate the longitudinal antidamping-like field (H_{DL}) and the transverse field-like field (H_{FL}), respectively, as in Ref. 33. Figures 3(a) and 3(b) show the results of harmonic Hall voltage measurements for the Ta/Pt/Co/Ta-20 film for the field along the current flow and the field perpendicular to the current, respectively. Figures 3(c) and 3(d) show the numerical fits (blue curves) of the V_{2f} data (red squares).[33] The fitting yielded $H_{DL} = 42.25$ Oe and $H_{FL} = -5.46$ Oe. Based on these values, an effective SHA of 0.62 was estimated for the Ta/Pt/Co/Ta-20 film; this value is consistent with the one (0.61) obtained from the above DC Hall measurements. Furthermore, the fitting analysis also yielded $H^0_{an} = 9900$ Oe, which is in agreement with the one obtained from the DC Hall method [see Fig. 2(d)].

Several notes should be made about the above discussions. First, the above-described H^0_{an} and Θ^{eff}_{SH} values are higher than the corresponding values in the other three samples. For example, the Ta/Pt/Co/Ta sample prepared under $P_{Ar} = 10$ mTorr (labeled as Ta/Pt/Co/Ta-10) shows $H^0_{an} = 5942$ Oe and $\Theta^{eff}_{SH} = 0.39$ at 300 K (see Fig. S3 in the supplementary material), both notably lower than the values in the Ta/Pt/Co/Ta-20 sample. Second, our harmonic Hall measurements indicate that the damping-like torque in our sample is stronger than the field-like torque.[19,32] For this reason, the above analysis based on the DC Hall method has neglected the field-like torque and has

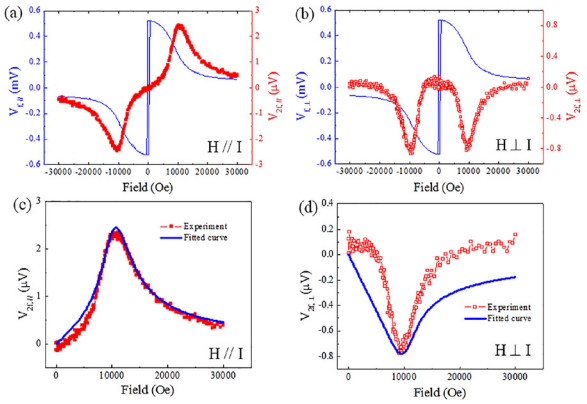

FIG. 3. First (V_f) and second (V_{2f}) harmonic loops of the Ta/Pt/Co/Ta-20 sample in (a) longitudinal (H//I) and (b) transverse (H ⊥ I) configurations, measured at 300 K. The fitting of second harmonic voltage curves in (c) longitudinal and (d) transverse configurations.

considered the damping-like torque only, as in previous works.[34,35] Third, in our samples, the contribution from the anomalous Nernst effect (ANE) is negligibly small and can be neglected[34,36] (see S4 in the supplementary material). Fourth, using $K_{eff} = H_{an} \cdot M_S/2$, the effective anisotropy constants (K_{eff}) of the Ta/Pt/Co/Ta-20 and Ta/Pt/Co/Ta-10 samples were estimated to be 5.9×10^6 and 3.7×10^6 erg/cm^3, respectively. Finally, the above switching efficiency (η) evaluation used the PMA field presented in Fig. 2(d).

Figure 4 shows the typical Co $L_{2,3}$ XAS data of the Ta/Pt/Co/Ta-20 and Ta/Pt/Co/ Ta-10 samples. One usually defines the XAS branching ratio B as the fraction of the total XAS intensity I in the L_3 edge, i.e., $B = I(L_3)/[I(L_3)+I(L_2)]$. Theoretically, one has $B = B_0 + (\langle l \cdot s \rangle / n_h)$, where B_0 is a constant representing the branching ratio in the absence of the spin-orbit interaction, l is the orbital angular momentum, s is the spin angular momentum, and n_h is the number of d holes. Thus, $(B-B_0)$ is proportional to the ground-state expectation value of the angular part of the spin-orbit interaction per Co 3d hole.[37] It provides a direct measure of interfacial SOC in FM/HM structures. The analysis of the data shown in Fig. 4 yields $B = 0.78 \pm 0.01$ for the Ta/Pt/Co/Ta-20 sample and $B = 0.75 \pm 0.01$ for the Ta/Pt/Co/Ta-10 sample. The higher B value in the Ta/Pt/Co/Ta-20 sample indicates a stronger interfacial SOC.[38] This result is in line with the theoretical prediction by Wang *et al.*[25] about the important contributions

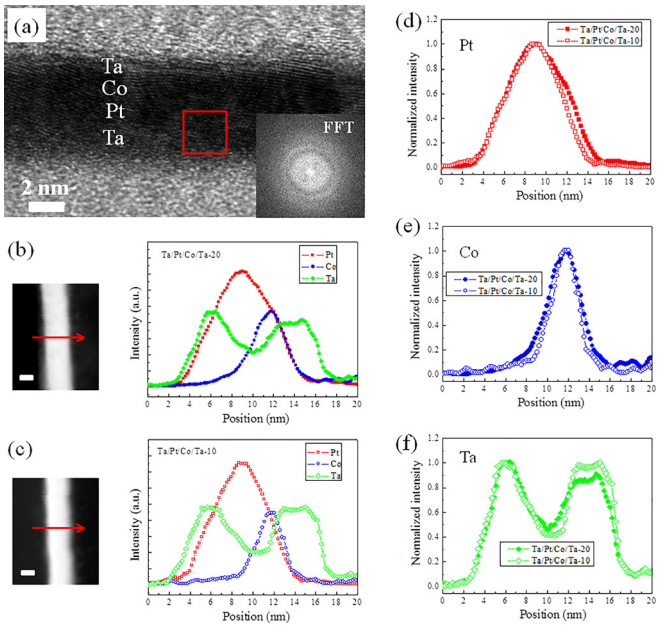

FIG. 5. (a) Cross-sectional HRTEM image of the Ta/Pt/Co/Ta-20 sample. The inset shows the diffractograms computed by FFT of the area indicated by the red square. (b) and (c) Cross-sectional HAADF-STEM images and EDX line scan profiles of Ta/Pt/Co/Ta-20 (b) and Ta/Pt/Co/Ta-10 (c). The EDX line scans are along the red arrows. The size of the white bars is 5 nm. (d)–(f) Normalized EDX line scan profiles of Pt, Co, and Ta which are obtained from the data in (b) and (c).

of the interfacial spin-orbit interaction in HM/FM structures to the PMA and the effective SHA.

Figure 5 gives the cross-sectional high-resolution TEM (HRTEM) images and the HAADF-STEM data of the two samples. One can see from Fig. 5(a) that the Ta and Pt layers in the Ta/Pt/Co/Ta-20 sample seem to be amorphous. The corresponding fast Fourier transform (FFT) of the area indicated by a red square is obtained and is given in the inset of Fig. 5(a). The ring like diffraction pattern verifies that the Ta and Pt layers are amorphous-like. This phenomenon is related to interfacial diffusion between the layers, as reported previously.[39,40] The EDX line scan data show that both the samples show significant overlap of Pt, Co, and Ta signals, indicating intermixing between those elements. The normalized signal intensity patterns of Pt, Co, and Ta shown in Figs. 5(d)–5(f) are obviously different for the two samples. The broader peak profiles of the Ta/Pt/Co/Ta-20 sample suggest more

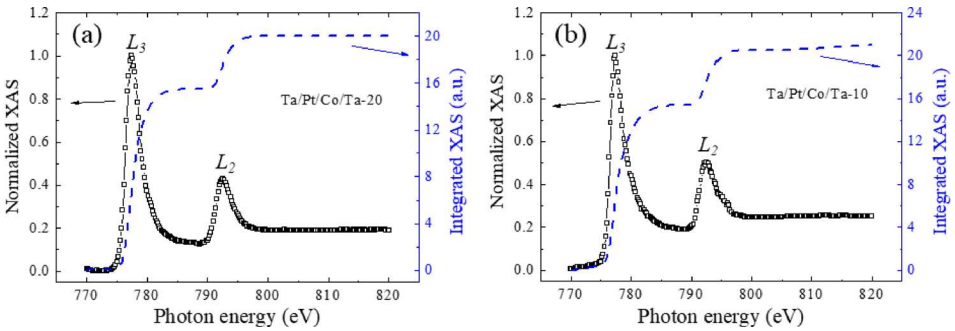

FIG. 4. Co $L_{2,3}$ XAS of (a) Ta/Pt/Co/Ta-20 and (b) Ta/Pt/Co/Ta-10 samples. The dashed lines show the integrated intensities, which are used to obtain the branching ratio B.

significant interfacial diffusion between the Co and the HMs in the sample than that in the Ta/Pt/Co/Ta-10 sample. In general, the incorporation of Co atoms in HMs can induce extrinsic SOC at the interfaces;[41–43] the Co atoms in the Pt and Ta layers can work as magnetic scattering centers and thereby result in enhanced PMA and SHA.

In this work, we demonstrate enhanced PMA and SOT in a Ta/Pt/Co/Ta structure where the two HM layers adjacent to the Co layer have opposite spin Hall angles (SHAs). The PMA field H_{an}^{0} exceeds 9000 Oe at 300 K and 14000 Oe at 10 K. This strong PMA property is highly desired in terms of maintaining a sufficiently large energy barrier against thermal fluctuation. The effective SHA value reaches 0.61 ± 0.03, which is larger than the values reported previously for Pt(Ta)-based tri-layered systems. The SOT-driven switching was demonstrated, and the critical switching current density is on the order of 10^6 A/cm^2. XAS and HAADF-STEM analyses suggest that the demonstrated PMA and SOT efficiency enhancement originates from enhanced SOC at the interfaces due to interfacial diffusion during the sample growth. Our results suggest that interface control can provide a powerful means to obtain strong PMA and large SHA for applications in high-density, high-efficiency SOT devices.

See supplementary material for the out-of-plane hysteresis loops of the four samples at 300 K, the calculation of the PMA field of the Ta/Pt/Co/Ta-20 sample, the calculation of H_{an} and SHA in the Ta/Pt/Co/Ta-10 film, the anomalous Nernst effect, and atomic force microscopy images.

The authors thank Xuepeng Qiu and Huanglin Yang (Tongji University) for performing the harmonic Hall voltage measurements. This work was financially supported by the NSFC (Nos. 51571136, 61434002, and 51871137). M.W. acknowledges the support from the U.S. National Science Foundation (EFMA1641989) and the U.S. Department of Energy, Office of Science, Basic Energy Sciences (DE-SC-0018994). The authors also acknowledge Beamline BL08U1A (Shanghai Synchrotron Radiation Facility, Shanghai, China) and Beamline BL12-a (National Synchrotron Radiation Laboratory, Hefei, China) stations for XAS measurements.

REFERENCES

[1]A. Brataas, A. D. Kent, and H. Ohno, Nat. Mater. **11**(5), 372 (2012).
[2]A. Soumyanarayanan, N. Reyren, A. Fert, and C. Panagopoulos, Nature **539**(7630), 509 (2016).
[3]L. Liu, C.-F. Pai, Y. Li, H. W. Tseng, D. C. Ralph, and R. A. Buhrman, Science **336**, 555 (2012).
[4]L. Liu, O. J. Lee, T. J. Gudmundsen, D. C. Ralph, and R. A. Buhrman, Phys. Rev. Lett. **109**(9), 096602 (2012).
[5]P. Li, T. Liu, H. Chang, A. Kalitsov, W. Zhang, G. Csaba, W. Li, D. Richardson, A. DeMann, G. Rimal, H. Dey, J. S. Jiang, W. Porod, S. B. Field, J. Tang, M. C. Marconi, A. Hoffmann, O. Mryasov, and M. Wu, Nat. Commun. **7**, 12688 (2016).
[6]G. Y. Shi, C. H. Wan, Y. S. Chang, F. Li, X. J. Zhou, P. X. Zhang, J. W. Cai, X. F. Han, F. Pan, and C. Song, Phys. Rev. B **95**(10), 104435 (2017).
[7]P. P. Haazen, E. Murè, J. H. Franken, R. Lavrijsen, H. J. M. Swagten, and B. Koopmans, Nat. Mater. **12**(4), 299 (2013).
[8]S. Emori, U. Bauer, S. M. Ahn, E. Martinez, and G. S. D. Beach, Nat. Mater. **12**(7), 611 (2013).
[9]V. E. Demidov, S. Urazhdin, H. Ulrichs, V. Tiberkevich, A. Slavin, D. Baither, G. Schmitz, and S. O. Demokritov, Nat. Mater. **11**(12), 1028 (2012).
[10]L. Liu, C.-F. Pai, D. C. Ralph, and R. A. Buhrman, Phys. Rev. Lett. **109**(18), 186602 (2012).
[11]S. Ikeda, K. Miura, H. Yamamoto, K. Mizunuma, H. D. Gan, M. Endo, S. Kanai, J. Hayakawa, F. Matsukura, and H. Ohno, Nat. Mater. **9**(9), 721 (2010).
[12]D. C. Worledge, G. Hu, D. W. Abraham, J. Z. Sun, P. L. Trouilloud, J. Nowak, S. Brown, M. C. Gaidis, E. J. O'Sullivan, and R. P. Robertazzi, Appl. Phys. Lett. **98**(2), 022501 (2011).
[13]J. Sinha, M. Hayashi, A. J. Kellock, S. Fukami, M. Yamanouchi, H. Sato, S. Ikeda, S. Mitani, S. Yang, S. S. P. Parkin, and H. Ohno, Appl. Phys. Lett. **102**(24), 242405 (2013).
[14]Y. Ou, D. C. Ralph, and R. A. Buhrman, Appl. Phys. Lett. **110**(19), 192403 (2017).
[15]T. Nozaki, T. Yamamoto, S. Tamaru, H. Kubota, A. Fukushima, Y. Suzuki, and S. Yuasa, APL Mater. **6**(2), 026101 (2018).
[16]M. Morota, Y. Niimi, K. Ohnishi, D. H. Wei, T. Tanaka, H. Kontani, T. Kimura, and Y. Otani, Phys. Rev. B **83**(17), 174405 (2011).
[17]A. Hoffmann, IEEE Trans. Magn. **49**, 5172 (2013).
[18]K.-S. Lee, S.-W. Lee, B.-C. Min, and K.-J. Lee, Appl. Phys. Lett. **102**(11), 112410 (2013).
[19]S. Woo, M. Mann, A. J. Tan, L. Caretta, and G. S. D. Beach, Appl. Phys. Lett. **105**(21), 212404 (2014).
[20]J. Yu, X. Qiu, W. Legrand, and H. Yang, Appl. Phys. Lett. **109**(4), 042403 (2016).
[21]C.-F. Pai, M.-H. Nguyen, C. Belvin, L. H. Vilela-Leão, D. C. Ralph, and R. A. Buhrman, Appl. Phys. Lett. **104**(8), 082407 (2014).
[22]W. Zhang, W. Han, X. Jiang, S.-H. Yang, and S. S. P. Parkin, Nat. Phys. **11**(6), 496 (2015).
[23]X. Qiu, Z. Shi, W. Fan, S. Zhou, and H. Yang, Adv. Mater. **30**(17), 1705699 (2018).
[24]B. Cui, S. Chen, D. Li, J. Yun, X. Guo, K. Wu, X. Zhang, Y. Wang, Y. Zuo, M. Gao, and L. Xi, Appl. Phys. Express **11**(1), 013001 (2018).
[25]L. Wang, R. J. H. Wesselink, Y. Liu, Z. Yuan, K. Xia, and P. J. Kelly, Phys. Rev. Lett. **116**(19), 196602 (2016).
[26]R. Ramaswamy, X. Qiu, T. Dutta, S. D. Pollard, and H. Yang, Appl. Phys. Lett. **108**(20), 202406 (2016).
[27]Y. Liu, Y. Liu, K. Cai, L. Ren, Y. Zheng, H. Yang, and K. L. Teo, IEEE Trans. Magn. **54**, 2600104 (2018).
[28]K. Cai, M. Yang, H. Ju, S. Wang, Y. Ji, B. Li, K. W. Edmonds, Y. Sheng, B. Zhang, N. Zhang, S. Liu, H. Zheng, and K. Wang, Nat. Mater. **16**, 712 (2017).
[29]Q. Hao and G. Xiao, Phys. Rev. B **91**(22), 224413 (2015).
[30]L. Neumann, D. Meier, J. Schmalhorst, K. Rott, G. Reiss, and M. Meinert, Appl. Phys. Lett. **109**(14), 142405 (2016).
[31]S. Emori, U. Bauer, S. Woo, and G. S. D. Beach, Appl. Phys. Lett. **105**(22), 222401 (2014).
[32]D. Li, B. Cui, T. Wang, J. Yun, X. Guo, K. Wu, Y. Zuo, J. Wang, D. Yang, and L. Xi, Appl. Phys. Lett. **110**(13), 132407 (2017).
[33]X. Qiu, P. Deorani, K. Narayanapillai, K.-S. Lee, K.-J. Lee, H.-W. Lee, and H. Yang, Sci. Rep. **4**, 4491 (2014).
[34]C. O. Avci, K. Garello, M. Gabureac, A. Ghosh, A. Fuhrer, S. F. Alvarado, and P. Gambardella, Phys. Rev. B **90**(22), 224427 (2014).
[35]C. O. Avci, K. Garello, A. Ghosh, M. Gabureac, S. F. Alvarado, and P. Gambardella, Nat. Phys. **11**(7), 570 (2015).
[36]K. Garello, I. M. Miron, C. O. Avci, F. Freimuth, Y. Mokrousov, S. Blügel, S. Auffret, O. Boulle, G. Gaudin, and P. Gambardella, Nat. Nanotechnol. **8**, 587 (2013).
[37]B. T. Thole and G. van der Laan, Phys. Rev. B **38**(5), 3158 (1988).
[38]J. W. Lee, Y.-W. Oh, S.-Y. Park, A. I. Figueroa, G. van der Laan, G. Go, K.-J. Lee, and B.-G. Park, Phys. Rev. B **96**(6), 064405 (2017).
[39]Z. B. Guo, W. B. Mi, R. O. Aboljadayel, B. Zhang, Q. Zhang, P. G. Barba, A. Manchon, and X. X. Zhang, Phys. Rev. B **86**(10), 104433 (2012).
[40]J. Liu, T. Ohkubo, S. Mitani, K. Hono, and M. Hayashi, Appl. Phys. Lett. **107**(23), 232408 (2015).
[41]G. Y. Guo, S. Maekawa, and N. Nagaosa, Phys. Rev. Lett. **102**(3), 036401 (2009).
[42]B. Gu, J.-Y. Gan, N. Bulut, T. Ziman, G. Y. Guo, N. Nagaosa, and S. Maekawa, Phys. Rev. Lett. **105**(8), 086401 (2010).
[43]P.-C. Chen, Y. Du, B.-Y. Yang, P.-H. Lin, G.-Y. Guo, M. Pakala, and C.-H. Lai, Phys. Rev. Mater. **2**(6), 064408 (2018).